



# Dispersion-tailored few-mode fiber design for tunable microwave photonic signal processing

ELHAM NAZEMOSADAT\*  AND IVANA GASULLA 

*ITEAM Research Institute, Universitat Politècnica de València, Camino de Vera, 46022 Valencia, Spain*

\**sbnazars@iteam.upv.es*

**Abstract:** We present a novel double-clad step-index few-mode fiber that operates as a five-sampled tunable true-time delay line. The unique feature of this design lies in its particular modal chromatic dispersion behavior, which varies in constant incremental steps among adjacent groups of modes. This property, which to the best of our knowledge has not been reported in any other few-mode fiber to date, is the key to tunable operation of radiofrequency signal processing functionalities implemented in few-mode fibers. The performance of the designed true-time delay line is theoretically evaluated for two different microwave photonics applications, namely tunable signal filtering and optical beamforming networks for phased array antennas. In the 35-nm optical wavelength tuning range of the C-band, the free spectral range of the microwave filter and the beam-pointing angle in the phased array antenna can be continuously tuned from 12.4 up to 57 GHz and 12.6° up to 90°, respectively.

© 2020 Optical Society of America under the terms of the [OSA Open Access Publishing Agreement](#)

## 1. Introduction

Space-division multiplexing (SDM) provides a promising approach to overcome the capacity limit of conventional single-mode fiber networks [1]. In this technology, the network capacity is increased by transmitting data over individual cores of a multicore fiber (MCF) [2], orthogonal spatial modes of a few-mode fiber (FMF) [3] or a combination of both [4]. Beyond optical transmission, MCFs and FMFs have found applications in sensing [5], medical imaging [6], all-optical nonlinear processing [7–9], astrophotonics [10], and microwave photonics (MWP) [11–19], amongst others.

The application of SDM fibers in microwave photonics lies in their ability to operate as optical sampled true-time delay lines (TTDLs), which are the building blocks of many signal processing functionalities based on discrete-time incoherent architectures, such as signal filtering, optical beam-steering in phased-array antennas and arbitrary waveform generation [20,21]. TTDLs provide a set of time-delayed samples of a radiofrequency (RF) signal, where the differential time delay between adjacent samples is constant. Such delay lines have been implemented in single-mode fibers using different approaches, including dispersive fibers [22,23], fiber Bragg gratings (FBGs) [24] and the nonlinear stimulated Brillouin scattering effect [25]. Moreover, the different spatial paths propagating in an SDM fiber can also provide equally-spaced time-delayed samples of an RF signal, given that each path generally features a distinct group delay and chromatic dispersion. TTDLs have been explored in different SDM fibers, including homogeneous MCFs [26,27], heterogeneous MCFs [11,12], multicore photonic crystal fibers [13] and FMFs [14–19]. One of the advantages brought by the use of SDM-based TTDLs is that they offer sample diversity in two dimensions, namely space and optical wavelength. In the spatial diversity, time-delayed samples are generated by a given optical wavelength propagating in distinct spatial paths (cores or modes), while the wavelength diversity takes advantage of the time delay experienced by different wavelengths propagating in a given spatial path. Figure 1 depicts this concept for a FMF-based TTDL.

The inherent parallelism of SDM fibers is beneficial to MWP signal processing, as it offers increased compactness as well as performance flexibility and versatility, providing a simple

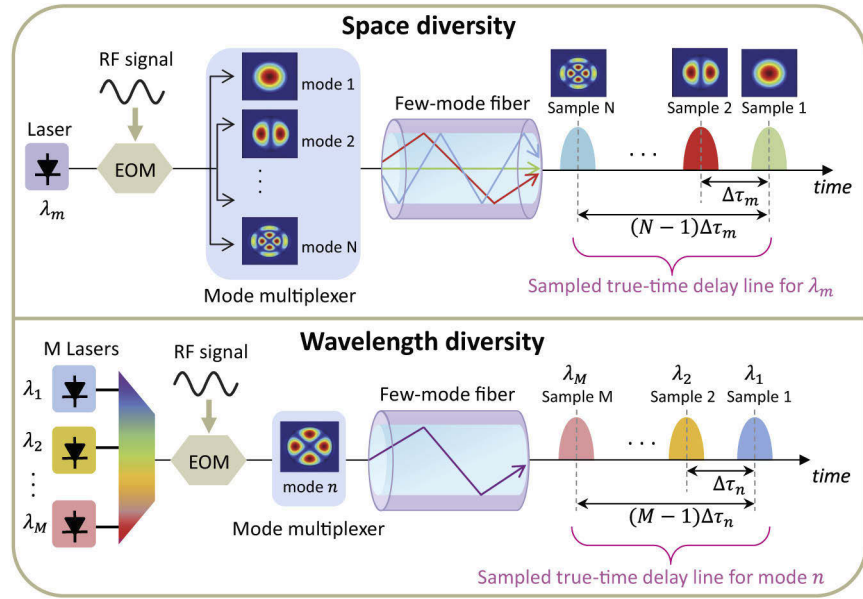


**Fig. 1.** Sampled true-time delay line realized by exploiting the spatial and wavelength diversities of a FMF. EOM: electro-optic modulator.

approach for fiber-distributed signal processing along short- and medium-reach distances. Additionally, FMFs provide an extra advantage, as they benefit from a simpler and more cost-effective fabrication process as compared to MCFs. Several studies have explored the implementation of TTDLs over FMFs; however, they have limitations either in their tunability (operate only at a single wavelength [15–17] or practically exhibit a wavelength-independent time delay [14,19]), number of samples [14], or complexity of the structure due to inscription of long period gratings [16–18]. In this work, we present a novel yet simple dispersion-engineered double-clad step-index FMF design that addresses all these issues. The proposed FMF offers, for the first time to the best of our knowledge, continuously tunable TTDL operation in both space and wavelength diversity domains. In the spatial diversity, 5 samples are provided by the modes LP<sub>01</sub>, LP<sub>11</sub>, LP<sub>21</sub>, LP<sub>31</sub> and LP<sub>41</sub>. This feasible design is a promising platform for implementing reconfigurable RF signal processing functionalities, specially along short-reach (in the order of 1 km) radio-over-fiber links, such as those encountered in 5G radio access networks.

## 2. Basic FMF requirements to operate as a tunable TTDL

For a given spatial mode  $n$ , the group delay,  $\tau_n$ , at an optical wavelength  $\lambda$ , can be expanded in a Taylor series around a reference wavelength  $\lambda_0$ , as:

$$\tau_n(\lambda) = [\tau_{0,n} + D_{0,n}(\lambda - \lambda_0) + \frac{1}{2}S_{0,n}(\lambda - \lambda_0)^2]L, \quad (1)$$

where  $\tau_{0,n}$ ,  $D_{0,n}$  and  $S_{0,n}$  are the group delay per unit length, chromatic dispersion and dispersion slope of mode  $n$  at  $\lambda_0$ , respectively, and  $L$  is the fiber length. The differential group delay (DGD) between adjacent modes  $n$  and  $n + 1$ , in the spatial diversity regime, is then given by:

$$\Delta\tau_{n,n+1}(\lambda) = [\Delta\tau_0 + \Delta D(\lambda - \lambda_0) + \frac{1}{2}(S_{0,n+1} - S_{0,n})(\lambda - \lambda_0)^2]L \approx [\Delta\tau_0 + \Delta D(\lambda - \lambda_0)]L, \quad (2)$$

where  $\Delta\tau_0 = \tau_{0,n+1} - \tau_{0,n}$  and  $\Delta D = D_{0,n+1} - D_{0,n}$  are the differential group delay and differential chromatic dispersion between adjacent modes at the reference wavelength. Since in typical FMFs,

$S_{0,n+1} - S_{0,n}$  is in the order of  $1 \times 10^{-3}$  ps/nm<sup>2</sup>/km, the third term in Eq. (2) is orders of magnitude smaller than the other terms and can be neglected when operating in the optical C-band.

When exploiting the wavelength diversity, a given mode  $n$  is fed by  $M$  optical laser sources. Thus, the DGD between any two neighboring wavelengths  $\lambda_m$  and  $\lambda_{m+1}$  ( $1 \leq m \leq M - 1$ ), is:

$$\Delta\tau_n(\lambda_m, \lambda_{m+1}) = [D_{0,n}\delta\lambda + S_{0,n}(\lambda_1 - \lambda_0)\delta\lambda + S_{0,n}(m - \frac{1}{2})\delta\lambda^2]L, \quad (3)$$

where  $\delta\lambda = \lambda_{m+1} - \lambda_m$  is the wavelength spacing between the adjacent optical sources and  $\lambda_1$  is the wavelength of the first optical source. Proper operation of a TTDL requires a constant  $\Delta\tau$  value among any two adjacent samples. As observed in Eq. (3), when operating in the wavelength diversity domain,  $\Delta\tau$  only depends on  $D_{0,n}$  and  $S_{0,n}$  of the particular mode that is used and is not affected by the dispersion properties of the other modes. Hence, distinct TTDLs can be realized in any given FMF, when the wavelength diversity of the FMF is exploited. However, when operating in the space diversity domain, as seen in Eq. (2),  $\Delta\tau$  depends on the differential dispersion properties of all involved modes. Consequently, one can not realize a TTDL by exploiting the space diversity of a given FMF, unless the FMF is suitably designed in terms of its modal dispersion characteristics. Therefore, to be able to take advantage of both diversity operation regimes, in what follows, we will focus on designing tunable FMF-based TTDLs that can also be implemented in the space diversity.

To enable TTDL operation at a given wavelength in the space diversity,  $\Delta\tau$  value among any two adjacent modes should be constant. Moreover, if this condition holds over a wavelength range instead of a single wavelength, a continuously tunable TTDL can be obtained. Thus, according to Eq. (2), a FMF should fulfill two requirements in order to operate as a tunable TTDL, i.e., to have a (i) constant differential group delay  $\Delta\tau_0$  and a (ii) constant differential chromatic dispersion  $\Delta D$  between adjacent modes, at the reference wavelength. It should be noted that the adjacent samples of the TTDL do not necessarily have to belong to adjacent eigenmodes of the FMF. As a matter of fact, those adjacent modes that are within one mode-group generally have quite similar dispersion characteristics and therefore do not fulfill the requirements to operate as a tunable TTDL. In this case, modes within adjacent mode-groups should be considered instead. Hereafter, unless otherwise stated, when referring to adjacent modes, we refer to any two neighboring modes within a particular set of modes that satisfy the two necessary requirements of a tunable TTDL.

To date, none of the reported FMFs operating as TTDLs have a constant  $\Delta D$  and therefore they are not tunable with the optical wavelength. Nonetheless, even with a constant  $\Delta D$ , one must still overcome an issue to be able to achieve tunable delay lines. In FMFs,  $\Delta D$  is typically several orders of magnitude smaller than  $\Delta\tau_0$ . Therefore, the contribution of the second term in the right-hand side of Eq. (2) becomes insignificant, which leads to a TTDL with low tunability. In MWP, however, tunable TTDLs are of higher interest as they increase the reconfigurability of the signal processing functionalities. A feasible solution to the tunability problem is to reduce  $\Delta\tau_0$  to a value comparable to  $\Delta D$ , so that both terms in Eq. (2) contribute to the DGD similarly and consequently a tunable delay line is realized. This could be implemented by using simple external delay lines (short lengths of single-mode fiber) at the FMF output, after the demultiplexer, to adjust the DGD of the modes at  $\lambda_0$ , while maintaining the chromatic dispersion behavior of every FMF mode. By using an individual external delay line for each mode, the DGD can be adjusted such that  $\Delta\tau_0$  among any two adjacent modes is decreased to the same order as  $\Delta D$ . In the meantime, it should also be made sure that  $\Delta\tau$  is constant between adjacent modes. This allows us to easily fulfill the aforementioned requirement (i), even if the original DGDs between adjacent modes are not constant. This means that, when designing a FMF to be used as a tunable TTDL, without being concerned about the DGD, one has to only optimize the fiber structure such that adjacent modes exhibit a constant and as large as possible  $\Delta D$  (requirement (ii)). It is worth mentioning that it is sufficient to externally adjust the DGD for only one particular wavelength ( $\lambda_0$  in our case), without needing to re-adjust it for a different operating wavelength. The reason

is that according to Eq. (2), when both  $\Delta\tau_0$  and  $\Delta D$  are constant for a particular wavelength, then one can obtain a constant  $\Delta\tau$  over a broad wavelength range.

### 3. Design of FMF with constant $\Delta D$ among adjacent modes

As described above, the FMF should have a constant and as large as possible  $\Delta D$ , in order to operate as a TTDL. Moreover, to suppress the mode coupling, macro-bend losses and nonlinearity in the FMF, three other conditions need to be met. A large differential effective refractive index,  $\Delta n_{\text{eff}}$ , is required between the modes to reduce the modal coupling, while a large relative effective refractive index difference with respect to the cladding,  $n_{\text{eff}} - n_{\text{cl}}$ , ensures low macro-bend losses [28]. Large effective mode areas,  $A_{\text{eff}}$ , are required to suppress nonlinearities in the FMF. For a fixed normalized frequency ( $V$  number), the mode coupling and bending losses could be reduced by increasing the differential refractive index between the core and cladding and decreasing the core radius. However, a small core radius leads to a small effective mode area and increases the nonlinearity. Hence, there is a trade-off between bending losses and mode coupling on one hand and nonlinearity on the other, which should be taken care of by properly selecting the core radius and refractive index [29].

To fulfill these conditions and meanwhile reduce the fabrication complexity and cost, we consider a FMF design with a step-index core. Since it is not possible to obtain a constant  $\Delta D$  between adjacent modes in a conventional step-index fiber, an inner cladding is added to the design, which alters the dispersion properties of the modes (particularly higher-order modes) and makes it possible to achieve a constant  $\Delta D$ . The refractive index profile of the proposed double-clad step-index fiber is shown in Fig. 2(a), where the silica core and inner cladding are doped with  $\text{GeO}_2$ . The fiber parameters  $\{a_1, n_1\}$  and  $\{a_2, n_2\}$ , corresponding to the radius and refractive index of the core and inner cladding, respectively, are optimized such that the relative standard deviation (RSD) of  $\Delta D$  is minimized at 1550 nm. This parameter is given by:

$$\text{RSD} = \frac{\sigma_{\Delta D}}{\overline{\Delta D}}, \quad (4)$$

where  $\sigma_{\Delta D}$  and  $\overline{\Delta D}$  are the standard deviation and mean value of  $\Delta D$  among adjacent modes, respectively. At a given wavelength, RSD compares the variations in  $\Delta D$  to its mean value and can be considered as an indication of the design error, showing how far the designed FMF is from having an ideal constant  $\Delta D$ . The smaller the RSD, the better the performance of the designed tunable TTDL. To calculate the dispersion properties of the FMF, the Sellmeier equation is used to describe the refractive index as a function of the wavelength [30]. The modal analysis is performed using the finite element method by COMSOL.

The optimum radii of the core and inner cladding are  $a_1 = 9.1 \mu\text{m}$  and  $a_2 = 13 \mu\text{m}$ , while their refractive indices at 1550 nm are  $n_1 = 1.456$  and  $n_2 = 1.453$ , respectively. The radius of the pure silica outer cladding is  $62.5 \mu\text{m}$ . Figure 2(a) displays the effective refractive index of the supported modes in the first five mode-groups. Five of these guided modes ( $\text{LP}_{01}$ ,  $\text{LP}_{11}$ ,  $\text{LP}_{21}$ ,  $\text{LP}_{31}$  and  $\text{LP}_{41}$ ), which belong to different mode-groups, have optimally spaced chromatic dispersion (constant  $\Delta D = 1.77 \text{ ps/nm/km}$  at 1550 nm) and fulfill the conditions to operate as a FMF-based TTDL. The transverse mode profiles of these modes are illustrated in Fig. 2(a), while their main characteristics are provided in Table 1.

The minimum  $\Delta n_{\text{eff}}$  between any of the modes of interest and any other guided mode in the FMF is  $0.4 \times 10^{-3}$ , which is between  $\text{LP}_{21}$  and  $\text{LP}_{02}$  within the third mode-group. This is comparable to the minimum  $\Delta n_{\text{eff}}$  value of typical commercial step-index FMFs ( $0.8 \times 10^{-3}$ ), which have been successfully used to demonstrate low crosstalk transmission over 40 km [29]. Furthermore, since  $\text{LP}_{02}$  is not one of the modes of interest, under ideal conditions it will not be excited at the FMF input or de-multiplexed at the output, so that it does not affect the TTDL operation. Since the modes of interest belong to different mode-groups, the minimum  $\Delta n_{\text{eff}}$

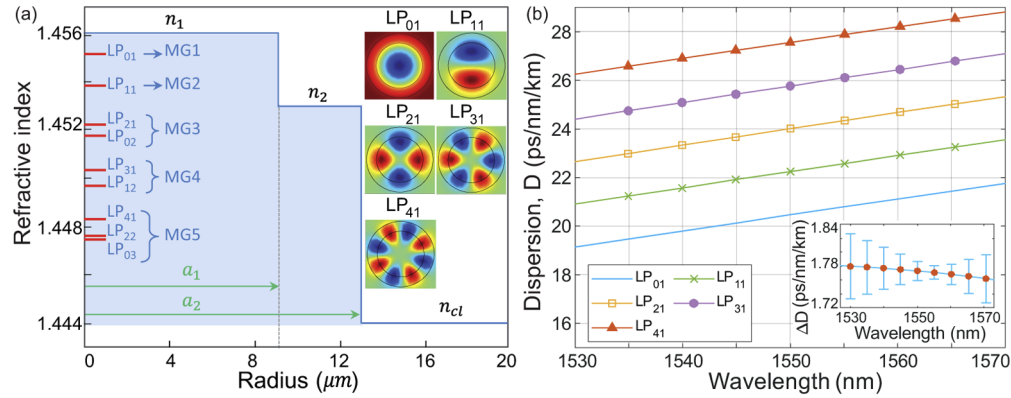


**Fig. 2.** (a) Refractive index profile of the designed double-clad step-index FMF. The red lines indicate the effective refractive index of the supported modes in the first five mode-groups (MGs), at 1550 nm. The transverse mode profiles of the 5 modes of interest that can operate as a tunable TTDL are demonstrated on the right. (b) Chromatic dispersion of the modes of interest. In the inset, the mean  $\Delta D$  values (red dots) and their associated error bars can be observed for different wavelengths.

**Table 1. Properties of the modes of interest at 1550 nm.**

	LP <sub>01</sub>	LP <sub>11</sub>	LP <sub>21</sub>	LP <sub>31</sub>	LP <sub>41</sub>
$(n_{\text{eff}} - n_{\text{cl}}) \times 10^{-3}$	11.1	9.8	8.2	6.3	4.3
$D$ (ps/nm/km)	20.47	22.25	24	25.77	27.56
DGD vs. LP <sub>01</sub> (ps/m)	0	2.33	4.84	7.29	9.65
$A_{\text{eff}}$ ( $\mu\text{m}^2$ )	213	314	356	393	425

between them is larger ( $1.3 \times 10^{-3}$ ) and therefore the chances of mode-coupling among them are lower. The large  $A_{\text{eff}}$  of all the modes (over  $200 \mu\text{m}^2$ ), ensures small intra- and inter-modal nonlinearity. For the modes of interest, the maximum intra-modal nonlinear coefficient belongs to LP<sub>01</sub> and is  $\gamma = 0.52 \text{ 1/(W.km)}$ , while that of the inter-modal case is between LP<sub>01</sub> and LP<sub>11</sub>, with a value of  $\gamma = 0.35 \text{ 1/(W.km)}$ .

The chromatic dispersion of the modes of interest is depicted in Fig. 2(b), as a function of the optical wavelength. The mean value of  $\Delta D$  (red dots) along with its corresponding standard deviation (error bar) at different wavelengths is shown in the inset. As can be observed, the maximum error in the C-band is at 1530 nm, which leads to an RSD of 2.6%. In the following section, it will be shown that this amount of error is tolerable and gives rise to an adequate response for different MWP signal processing applications. Thus,  $\Delta D$  in this fiber can be considered constant among the adjacent modes of interest over a broad wavelength range.

The DGD of the modes with respect to the group delay of LP<sub>01</sub> ( $\tau_{0,1}$ ) at  $\lambda_0 = 1520 \text{ nm}$  is shown in Fig. 3, while the inset displays the mean  $\Delta\tau$  value and its error bars. Comparison between the mean values of  $\Delta\tau$  and  $\Delta D$  (insets of Fig. 3 and Fig. 2(b)), shows that  $\Delta\tau$  is more than three orders of magnitude larger than  $\Delta D$ . Consequently, when such a TTDL operates in the C-band, the corresponding RF processing range (given by  $1/\Delta\tau$ ) of a given MWP application would be very limited in terms of tunability (see Eq. (2)). In the case of microwave signal filtering, the RF processing range corresponds to the free spectral range (FSR). To show the tunability limitation, we can consider a TTDL based on 40 cm of the designed FMF, which would result in a microwave signal filter with an FSR around 10.5 GHz at 1530 nm. In this case, tuning the wavelength over the entire C-band would only continuously tune the FSR of the filter for less



than 0.3 GHz. Thus, while such a TTDL can be used for a given MWP application with certain characteristics, it is not reconfigurable.

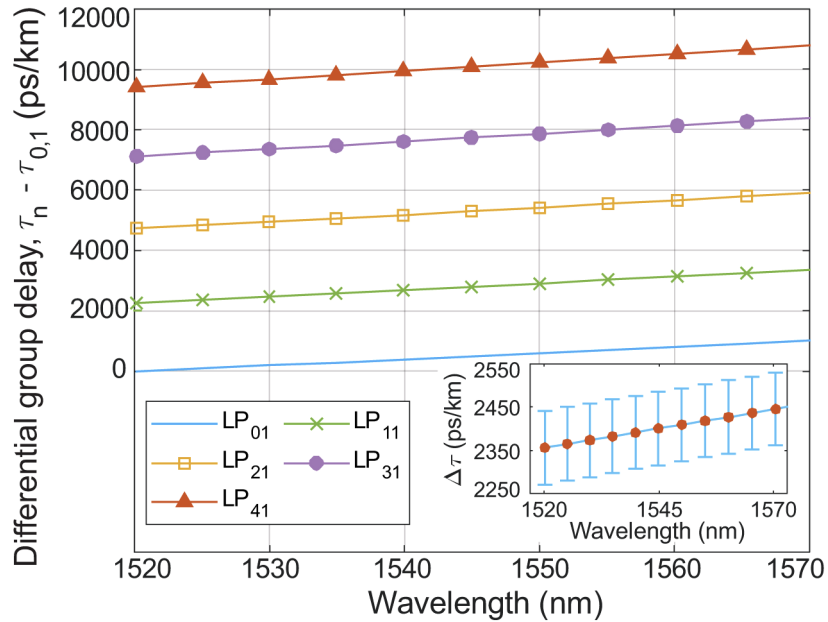


**Fig. 3.** Differential group delay per unit length between the modes of interest, with respect to LP<sub>01</sub> at 1520 nm. The inset shows the mean  $\Delta\tau$  value, which is around 2.4 ns/km at 1550 nm.

To solve this problem and realize tunable FMF-based TTDLs suitable for microwave signal processing, one can employ external delay lines at the output of the FMF. After demultiplexing the modes, individual external delay lines can be used for each mode to decrease  $\Delta\tau_0$ , without affecting the required chromatic dispersion behavior of the modes. In our case, we have adjusted the external delay lines such that  $\Delta\tau = 0$  is obtained at 1520 nm, as shown in Fig. 4(a). Subsequently, thanks to the constant  $\Delta D$ ,  $\Delta\tau$  varies linearly with the optical wavelength and a tunable TTDL for microwave signal processing is realized in the C-band. Figure 4(b) depicts the mean  $\Delta\tau$  after inserting the external delay lines, which has significantly decreased as compared to the case where external delay lines are not used (inset of Fig. 3). The corresponding FSR of a microwave filter realized based on 1-km of the proposed TTDL is displayed in Fig. 4(c), which confirms the tunability of the TTDL with the optical wavelength for MWP applications. For a 1-km FMF link, at  $\lambda_0 = 1520$  nm, the DGD of {LP<sub>01</sub>, LP<sub>11</sub>, LP<sub>21</sub>, LP<sub>31</sub> and LP<sub>41</sub>} modes with respect to the group delay of the slowest mode (LP<sub>41</sub>) are {9.42, 7.16, 4.7, 2.3, 0} ns, respectively, according to Fig. 3. Thus, to get  $\Delta\tau = 0$  at 1520 nm, the lengths of the single-mode fibers that are employed as external delay lines, should be {1.92, 1.46, 0.96, 0.47, 0} m, respectively. Such short single-mode fiber lengths have a negligible effect on the overall chromatic dispersion behavior of the fiber link and allow for a feasible implementation of a tunable TTDL using our designed FMF.

It should be noted that the large DGDs of the FMF are beneficial in terms of nonlinearity, as they limit the phase matching of inter-modal nonlinear processes [8,9]. Therefore, to avoid these nonlinear processes, it is better to place the external delay lines used for reducing the DGD, after the FMF and not before.

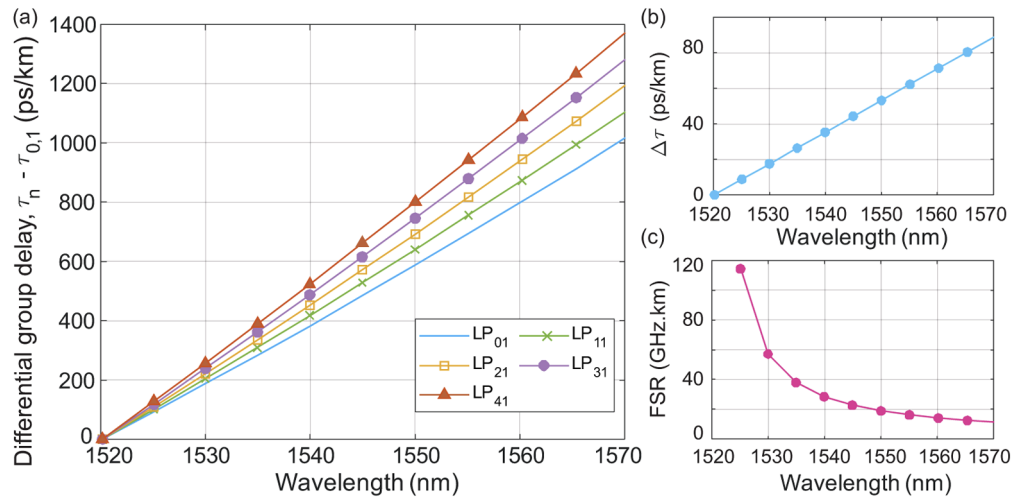


**Fig. 4.** (a) Differential group delay per unit length between the modes of interest, along with (b) their mean values, with respect to LP<sub>01</sub> at 1520 nm, after using external delay lines. As observed in (b), the mean  $\Delta\tau$  is around 53 ps/km at 1550 nm. Comparison between (b) and inset of Fig. 3, confirms that using the external delay lines notably reduces  $\Delta\tau$ . (c) Free spectral range of a microwave filter implemented over 1-km of the designed FMF.

#### 4. Performance in microwave signal processing applications

To verify the applicability of the designed TTDL in different MWP applications, we evaluate its performance over a 1-km FMF link, in two representative scenarios: tunable microwave signal filtering and optical beamforming for phased array antennas. In both applications, the time-delayed signal samples should first be demultiplexed at the FMF output. Thereafter, if the demultiplexed time-delayed samples are coupled together and detected with a single photodetector, a microwave signal filter could be realized [21], as shown in Fig. 5(a). On the other hand, if each of the demultiplexed samples is detected individually with a separate photodetector, a beamforming network for phased array antennas could be implemented, as depicted in Fig. 7(a), where each sample feeds a particular radiating element [31].

The calculated transfer function of the resulting 5-tap microwave filter with uniform tap coefficients, operating in the space diversity, as a function of the RF frequency, is shown in Fig. 5(b), for two different wavelengths. The filter response of an ideal FMF with a strictly constant  $\Delta\tau$  is also shown for reference. The time delay can be tuned from 80.4 to 17.5 ps within the C-band, which corresponds to continuously tuning the filter FSR from 12.4 GHz up to 57 GHz, when the optical source is tuned from 1565 nm to 1530 nm, respectively, validating the tunability of the designed TTDL. The main-to-sidelobe suppression ratio (MSSR) is around 12 dB in both cases, which could be further increased by applying windowing techniques, such as Hanning, Hamming or Blackman distributions [32].

From a practical point of view, while manufacturing a fiber, there is a high possibility that fabrication fluctuations occur and slightly vary the refractive index profile of the fiber. Such variations could modify the dispersion characteristics of the modes and result in unequal  $\Delta D$  values between consecutive mode-groups and therefore affect the performance of the FMF-based TTDL. To show the effect of such errors on the performance of the microwave filter, we have considered two particular cases where the core radius,  $a_1$ , and refractive index of the inner cladding,  $n_2$ , deviate from their optimal values by  $\pm 0.1 \mu\text{m}$  and  $\pm 0.0001$ , respectively. The resulting transfer functions are shown in Figs. 5(c) and (d). While an increase in the core radius

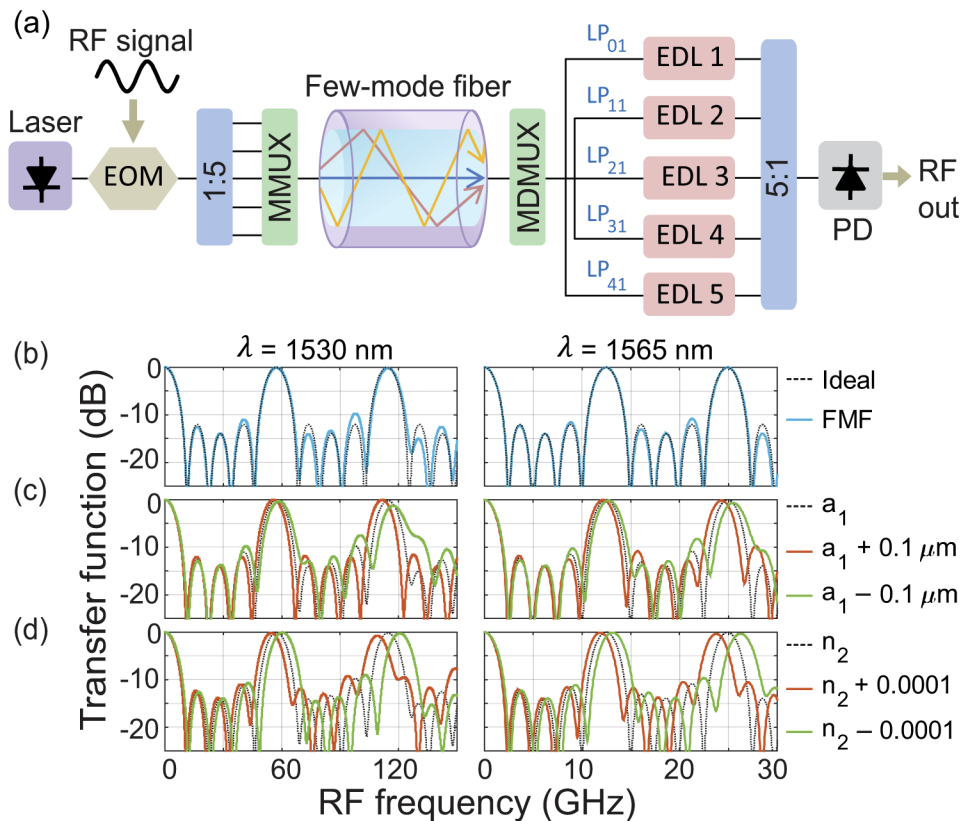


**Fig. 5.** (a) Implementation of a microwave signal filter operating in the space diversity, using the designed FMF. (b) Calculated normalized transfer function of a microwave signal filter that is realized with the proposed (solid line) and ideal (dotted line) 1-km FMF-based TTDL, at two different wavelengths. Performance of the signal filter, at 1530 nm and 1565 nm, with fabrication errors in the (c) core radius  $a_1$  and (d) inner cladding refractive index  $n_2$ . The dotted black curves correspond to the FMF without any fabrication errors. EOM: electro-optic modulator, MMUX: mode multiplexer, MDMUX: mode demultiplexer, EDL: external delay line, PD: photodetector.

does not affect the performance of the filter much, its reduction can degrade the performance, particularly at shorter wavelengths. As for variations in  $n_2$ , the filter performance is more sensitive to an increase in the refractive index as compared to a decrease. As observed, fabrication errors slightly shift the FSR of the filter, which is not a problem, since one can tune the FSR to a given desired value by simply changing the operating optical wavelength. Here, in Figs. 5(c) and (d), we have considered the cases where only the core or the inner cladding are affected by fabrication errors. However, it is more likely that if there are fabrication errors, both core and inner cladding will experience it simultaneously in a similar manner. In that case, the filter response is more robust to fluctuations and can tolerate up to  $\pm 0.4 \mu\text{m}$  and  $\pm 0.0006$  variations in the radii and refractive indices, respectively. Furthermore, possible mode coupling among the modes within one mode-group could affect the power levels of the samples, which in the frequency domain translates into slight variations in the filter bandwidth or MSSR. In the case of degenerate modes, given that they are strongly coupled, in principle they should be combined before or after photodetection in real application scenarios. This could be realized through employing optical or electrical diversity combining techniques if direct detection is used [33].



When the same FMF is fed by an array of 10 lasers, a 10-tap microwave filter can be realized by exploiting the wavelength diversity in each one of the fiber modes (Fig. 1). The frequency responses of such a filter, implemented over  $LP_{01}$  or  $LP_{41}$ , are shown in Fig. 6. These two modes have the lowest and highest chromatic dispersion values and consequently give rise to the highest and lowest FSRs, respectively. In Figs. 6(a)-(b) the wavelength spacing between the lasers is 1-nm, leading to maximum and minimum FSRs of 51.6 and 37.8 GHz, while in Figs. 6(c)-(d), the wavelength spacing is assumed 2-nm and the extreme FSR values drop to 25.2 and 18.5 GHz, accordingly. Thus, one can widely tune the microwave signal processing range by varying the number of optical lasers, the wavelength spacing between them or the mode in which the samples propagate in.

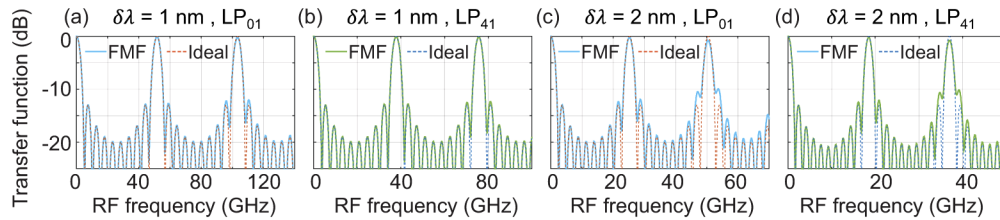


**Fig. 6.** Calculated normalized transfer function of a microwave signal filter realized with the proposed (solid line) and ideal (dotted line) 1-km FMF-based TTDL, when exploiting the wavelength diversity. A set of  $M = 10$  lasers with an initial wavelength of  $\lambda_1 = 1530$  nm are considered, where the separation between the lasers is (a)-(b) 1-nm and (c)-(d) 2-nm. The mode that is employed in (a),(c) is  $LP_{01}$ , while that of (b),(d) is  $LP_{41}$ .

To assess the performance of the TTDL in optical beamforming, when operating in space diversity, the array factor of the 5-element phased array antenna as a function of the beam-pointing angle, is calculated for different operating wavelengths and illustrated in Fig. 7(b). The spacing between radiating elements is assumed 2.4 cm, while the RF frequency is set to 6.2 GHz. The results indicate that by tuning the wavelength of the optical source from 1530 to 1565 nm, the beam-pointing angle of the antenna varies from  $12.6^\circ$  up to  $90^\circ$ .

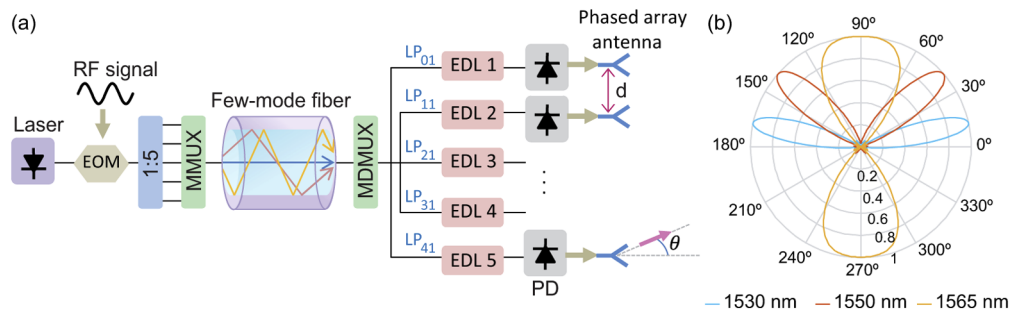


**Fig. 7.** (a) Implementation of an optical beamforming network using the designed FMF in space diversity operation. (b) Calculated array factor of the 5-element phased array antenna implemented using the proposed TTDL, for different operation wavelengths, for an RF frequency of 6.2 GHz and antenna element separation of  $d = 2.4$  cm. EOM: electro-optic modulator, MMUX: mode multiplexer, MDMUX: mode demultiplexer, EDL: external delay line, PD: photodetector.

## 5. Conclusions

Space-division multiplexed fibers are promising platforms for implementation of microwave photonics signal processing functionalities, as they can provide versatile fiber-distributed signal processing over a compact medium. Reconfigurable RF signal processing, which is highly desired in MWP, requires TTDLs in which the time delay can be continuously and widely tuned with the optical wavelength. FMF-based TTDLs usually do not inherit this feature within the RF processing ranges that are suitable for MWP applications, an aspect related to the inherent modal dispersion properties of FMFs. To overcome this limitation, we present a feasible solution comprising a novel double-clad step-index FMF design, featuring evenly-spaced incremental modal chromatic dispersion values, and insertion of external delay lines at the FMF output, to adjust the DGD among the modes at the anchor wavelength. The designed TTDL exhibits continuous tunability in both space and wavelength diversity operation domains, providing different TTDL configurations within the same link of fiber. When exploiting the spatial diversity, tunable five-sampled operation is realized by exciting five modes ( $LP_{01}$ ,  $LP_{11}$ ,  $LP_{21}$ ,  $LP_{31}$  and  $LP_{41}$ ), while distinct tunable TTDLs can be obtained with a variable number of samples (depending on the number of lasers involved), when using the wavelength diversity domain. The performance of the TTDL is studied in the context of reconfigurable microwave signal filtering and radio beam-steering in phased array antennas over a 1-km FMF link. Both applications demonstrate wide continuous tunability, as the microwave filter FSR can be tuned from 12.4 to 57 GHz and the beam-pointing angle of the phased array antenna can be tuned from  $12.6^\circ$  up to  $90^\circ$  over a 35-nm optical wavelength range. Beyond these scenarios, the applicability of the proposed TTDL can be extended to additional microwave signal processing functionalities, such as arbitrary waveform generation or multicavity-optoelectronic oscillation.

Fabrication of the designed dispersion-tailored FMF along with a suitable mode multiplexer and demultiplexer with low crosstalk, followed by experimental demonstrations of various microwave photonics signal processing applications, are our near future research plans in this field.

## Funding

European Research Council (Consolidator Grant Project 724663); Ministerio de Ciencia, Innovación y Universidades (Ramon y Cajal fellowship RYC-2014-16247).

## Disclosures

The authors declare no conflicts of interest.

## References

1. D. J. Richardson, J. M. Fini, and L. E. Nelson, "Space-division multiplexing in optical fibres," *Nat. Photonics* **7**(5), 354–362 (2013).
2. B. J. Puttnam, R. S. Luís, W. Klaus, J. Sakaguchi, J. Delgado Mendinueta, Y. Awaji, N. Wada, Y. Tamura, T. Hayashi, M. Hirano, and J. Marciano, "2.15 pb/s transmission using a 22 core homogeneous single-mode multi-core fiber and wideband optical comb," in *2015 European Conference on Optical Communication (ECOC)*, (2015), 1–3.
3. R. Ryf, S. Randel, A. H. Gnauck, C. Bolle, A. Sierra, S. Mumtaz, M. Esmacelpour, E. C. Burrows, R.-J. Essiambre, P. J. Winzer, D. W. Peckham, A. H. McCurdy, and R. Lingle, "Mode-division multiplexing over 96 km of few-mode fiber using coherent  $6 \times 6$  mimo processing," *J. Lightwave Technol.* **30**(4), 521–531 (2012).
4. K. Igarashi, D. Souma, Y. Wakayama, K. Takeshima, Y. Kawaguchi, T. Tsuritani, I. Morita, and M. Suzuki, "114 space-division-multiplexed transmission over 9.8-km weakly-coupled-6-mode uncoupled-19-core fibers," in *Optical Fiber Communication Conference Post Deadline Papers*, (Optical Society of America, 2015), p. Th5C.4.
5. Y. Liu and L. Wei, "Low-cost high-sensitivity strain and temperature sensing using graded-index multimode fibers," *Appl. Opt.* **46**(13), 2516–2519 (2007).
6. Y. Choi, C. Yoon, M. Kim, T. D. Yang, C. Fang-Yen, R. R. Dasari, K. J. Lee, and W. Choi, "Scanner-free and wide-field endoscopic imaging by using a single multimode optical fiber," *Phys. Rev. Lett.* **109**(20), 203901 (2012).
7. E. Nazemosadat and A. Mafi, "Nonlinear switching in a two-concentric-core chalcogenide glass optical fiber for passively mode-locking a fiber laser," *Opt. Lett.* **39**(16), 4675–4678 (2014).

8. Y. Xiao, R.-J. Essiambre, M. Desgroseilliers, A. M. Tulino, R. Ryf, S. Mumtaz, and G. P. Agrawal, "Theory of intermodal four-wave mixing with random linear mode coupling in few-mode fibers," *Opt. Express* **22**(26), 32039–32059 (2014).
9. J. Gao, E. Nazemosadat, C. Yang, S. Fu, M. Tang, W. Tong, J. Carpenter, J. Schröder, M. Karlsson, and P. Andrekson, "Design, fabrication, and characterization of a highly nonlinear few-mode fiber," *Photonics Res.* **7**(11), 1354–1362 (2019).
10. T. A. Birks, B. J. Mangan, A. Diez, J. L. Cruz, S. G. Leon-Saval, J. Bland-Hawthorn, and D. F. Murphy, "Multicore optical fibres for astrophotonics," in *CLEO/Europe and EQEC 2011 Conference Digest*, (Optical Society of America, 2011), p. JSIII2\_1.
11. I. Gasulla and J. Capmany, "Microwave photonics applications of multicore fibers," *IEEE Photonics J.* **4**(3), 877–888 (2012).
12. S. García, M. Ureña, and I. Gasulla, "Demonstration of distributed radiofrequency signal processing on heterogeneous multicore fibres," in *45th European Conference on Optical Communication (ECOC 2019)*, (2019), pp. 1–4.
13. S. Shaheen, I. Gris Sánchez, and I. Gasulla, "True-time delay line based on dispersion-flattened 19-core photonic crystal fiber," *J. Lightwave Technol.* **38**(22), 6237–6246 (2020).
14. K. H. Lee, W. Y. Choi, S. Choi, and K. Oh, "A novel tunable fiber-optic microwave filter using multimode DCF," *IEEE Photonics Technol. Lett.* **15**(7), 969–971 (2003).
15. D. V. Nickel, C. Villarruel, K. Koo, F. Bucholtz, and B. Haas, "Few Mode Fiber-Based Microwave Photonic Finite Impulse Response Filters," *J. Lightwave Technol.* **35**(23), 5230–5236 (2017).
16. R. Guillem, S. García, J. Madrigal, D. Barrera, and I. Gasulla, "Few-mode fiber true time delay lines for distributed radiofrequency signal processing," *Opt. Express* **26**(20), 25761 (2018).
17. S. García, R. Guillem, J. Madrigal, D. Barrera, S. Sales, and I. Gasulla, "Sampled true time delay line operation by inscription of long period gratings in few-mode fibers," *Opt. Express* **27**(16), 22787–22793 (2019).
18. S. García, R. Guillem, and I. Gasulla, "Ring-core few-mode fiber for tunable true time delay line operation," *Opt. Express* **27**(22), 31773–31782 (2019).
19. J. Zhao, H. Zhang, Z. Yang, J. Xu, T. Xu, and C. Wang, "Few-mode fibers with uniform differential mode group delay for microwave photonic signal processing," *IEEE Access* **8**, 135176–135183 (2020).
20. J. Yao, "Microwave Photonics," *J. Lightwave Technol.* **27**(3), 314–335 (2009).
21. J. Capmany, J. Mora, I. Gasulla, J. Sancho, J. Lloret, and S. Sales, "Microwave photonic signal processing," *J. Lightwave Technol.* **31**(4), 571–586 (2013).
22. K. Wilner and A. P. van den Heuvel, "Fiber-optic delay lines for microwave signal processing," *Proc. IEEE* **64**(5), 805–807 (1976).
23. D. Norton, S. Johns, C. Keefer, and R. Soref, "Tunable microwave filtering using high dispersion fiber time delays," *IEEE Photonics Technol. Lett.* **6**(7), 831–832 (1994).
24. D. B. Hunter and R. A. Minasian, "Microwave optical filters using in-fiber Bragg grating arrays," *IEEE Microw. Guid. Wave Lett.* **6**(2), 103–105 (1996).
25. A. Loayssa and F. J. Lahoz, "Broad-band RF photonic phase shifter based on stimulated Brillouin scattering and single-sideband modulation," *IEEE Photonics Technol. Lett.* **18**(1), 208–210 (2006).
26. I. Gasulla, D. Barrera, J. Hervás, and S. Sales, "Spatial division multiplexed microwave signal processing by selective grating inscription in homogeneous multicore fibers," *Sci. Rep.* **7**(1), 41727 (2017).
27. L. Huo, L. Gan, L. Shen, M. Tang, S. Fu, C. Yang, and W. Tong, "IIR microwave photonic filters based on homogeneous multicore fibers," *J. Lightwave Technol.* **36**(19), 4298–4304 (2018).
28. R. Olshansky, "Mode coupling effects in graded-index optical fibers," *Appl. Opt.* **14**(4), 935–945 (1975).
29. P. Sillard, M. Bigot-Astruc, D. Boivin, H. Maerten, and L. Provost, "Few-mode fiber for uncoupled mode-division multiplexing transmissions," in *37th European Conference and Exposition on Optical Communications*, (Optical Society of America, 2011), p. Tu.5.LeCervin.7.
30. J. W. Fleming, "Dispersion in GeO<sub>2</sub>-SiO<sub>2</sub> glasses," *Appl. Opt.* **23**(24), 4486–4493 (1984).
31. B. Ortega, J. L. Cruz, J. Capmany, M. V. Andres, and D. Pastor, "Variable delay line for phased-array antenna based on a chirped fiber grating," *IEEE Trans. Microwave Theory Tech.* **48**(8), 1352–1360 (2000).
32. A. V. Oppenheim, J. R. Buck, and R. W. Schaffer, *Discrete-Time Signal Processing*; 2nd ed. (Prentice-Hall, 1999).
33. I. Gasulla and J. M. Kahn, "Performance of direct-detection mode-group-division multiplexing using fused fiber couplers," *J. Lightwave Technol.* **33**(9), 1748–1760 (2015).